Chromosomal rearrangement-enhanced mRNA stability drives the oncogenic potential of fusion genes in pediatric leukemia

Xuejing Shao,[1,2] Zhimei Xia,[1] Minyi Cai,[1] Chen Shao,[1] Shaowei Bing,[1] Tianrui Wang,[1] Wenxin Du,[1] Jiayi Liu,[1] Diying Shen,[3] Ji Cao,[1] Bo Yang,[1,2,4] Qiaojun He,[1,2,5] Xiaojun Xu,[3] Jingying Zhang[3] and Meidan Ying[1-5]

[1]Institute of Pharmacology and Toxicology, Zhejiang Province Key Laboratory of Anti-Cancer Drug Research, College of Pharmaceutical Sciences, Zhejiang University; [2]Nanhu Brain-Computer Interface Institute; [3]Division of Hematology-Oncology, the Children's Hospital Zhejiang University School of Medicine; [4]School of Medicine, Hangzhou City University, Zhejiang and [5]Cancer Center, Zhejiang University, Hangzhou, China

Correspondence: M. Ying
mying@zju.edu.cn

J. Zhang
zhangjy423@zju.edu.cn

Received: May 19, 2025.
Accepted: November 7, 2025.
Early view: November 13, 2025.

https://doi.org/10.3324/haematol.2025.288256

©2026 Ferrata Storti Foundation
Published under a CC BY-NC license

Abstract

Acute lymphoblastic leukemia (ALL), the most common type of pediatric leukemia, is frequently driven by fusion genes generated by chromosomal rearrangements. Compared with wild-type genes, many oncogenic fusions show increased expression and sustained functional activity that drives tumorigenesis. However, the mechanisms by which chromosomal rearrangements lead to functional enhancement remain largely elusive. In addition, although large-scale sequencing has identified numerous fusion events, the functional significance of most remains unclear. Here, we demonstrate that enhanced mRNA stability represents an important tumorigenic mechanism for oncogenic fusions, including classical PAX5 fusions. Based on this mechanism, we characterize a novel oncogenic fusion, STK38-PXT1, which exhibits upregulated *STK38* mRNA levels and drives the development of ALL. Mechanistically, the increased mRNA stability results primarily from enhanced N6-methyladenosine modification of oncogenic fusions, which is attributable to "gene truncation" (as in *PAX5* fusions) and "partner collaboration" (as in *STK38-PXT1*). Furthermore, the m6A reader IGF2BP3 is crucial for maintaining the high mRNA stability of oncogenic fusions. We further propose venetoclax as an innovative and clinically available therapy for ALL driven by these oncogenic fusions characterized by high mRNA stability. Our study not only highlights mRNA stabilization as a crucial mechanism by which oncogenic fusions drive tumorigenesis, but also presents a promising therapeutic strategy for patients with ALL.

Introduction

Acute lymphoblastic leukemia (ALL) is the most common type of pediatric cancer and is a hematologic malignancy with multiple subtypes.[1,2] Clinically, it is categorized into genetically distinct subgroups mainly based on chromosomal rearrangement-induced specific gene fusions, such as *ETV6-RUNX1*, *PAX5* fusions, and so on.[3] Currently, chemotherapy is still used as the standard therapy, which poses significant long-term toxic risks such as cardiotoxicity.[4] While BCR-ABL1-targeted therapy exemplifies the success of fusion-driven treatment,[5,6] most ALL fusions lack effective targeted strategies. Elucidating the mechanism by which chromosome rearrangements lead to abnormal function of wild-type genes will help to put forward new targeted strategies.

The current focus of fusion research primarily lies in individual studies of each fusion,[7-10] leading to a lack of universality in research on carcinogenic mechanisms and intervention strategies. We ponder whether it is feasible to uncover a relatively universal oncogenic mechanism for fusions, which could potentially serve as a foundation for developing a generalized therapeutic strategy for intervening in different fusions. Meanwhile, although large-scale sequencing reveals many uncharacterized fusions in ALL,[11] their clinical relevance remains unclear. It is urgent to rapidly identify oncogenic fusions from complex events. Thus, we also wonder whether the identification of oncogenic fusions can be achieved based on this framework.

Protein function is precisely regulated at multiple levels, including transcription, post-transcriptional, translation,

and post-translational regulation. Compared to wild-type genes, various oncofusions exhibit continuously enhanced function to drive tumorigenesis. Several mechanisms have been suggested to account for the functional enhancement of oncogenic fusions. First, fusions such as P2RY8-CRLF2 can significantly activate transcription through promoter exchange, where the 5' untranslated region of *P2RY8* triggers the obvious transcriptional upregulation of *CRLF2*.[12] Second, fusion proteins such as MLL-AF9 are more stable than wild-type proteins due to the loss of post-translational ubiquitination.[13] Third, kinase fusions such as ABL, ALK and RET fusions exhibit sustained kinase activation by dimerization.[14] However, the underlying mechanism by which chromosomal rearrangements lead to functional enhancement still remains largely elusive. So far, the regulatory mechanisms of fusion proteins in post-transcriptional regulation, such as mRNA stability, have not been reported. The N6-methyladenosine (m6A) modification plays a pivotal role in modulating mRNA stability;[15] abnormal alterations in m6A methylation and its modulators (writers, erasers and readers) have been reported to be closely associated with cancer.[16,17] However, it remains completely unknown whether m6A modification regulates the mRNA stability of fusions, thereby participating in the tumorigenicity of oncofusions. In addition, the molecular events such as mRNA degradation and stabilization that occur through m6A modification rely on m6A readers.[18] Among them, YTH domain-containing proteins generally destabilize m6A-containing mRNA, whereas m6A-containing mRNA can be stabilized by other m6A reader proteins such as IGF2BP.[19,20] Based on these, we suspect that the mRNA stability regulated by the m6A modification would be a potential critical oncogenic mechanism for fusions, and m6A readers, especially those that can stabilize oncogenic fusions, may hold promise as therapeutic targets in cancer.

In this study, we propose a model for the first time suggesting that chromosomal rearrangements enhance mRNA stability of fusions to drive leukemogenesis, and identify a novel oncogenic fusion STK38-PXT1. Mechanistically, mRNA stability of oncofusions, including classical *PAX5* fusions and the new *STK38-PXT1*, increases due to enhanced m6A modification, mainly driven by gene truncation and partner collaborations. Furthermore, we propose venetoclax as a promising drug for the treatment of patients with oncofusion-driven ALL.

Methods

Fusions and gene expression of acute lymphoblastic leukemia samples

The fusion information and gene expression of 679 samples in TARGET ALL were supplied by the Therapeutically Applicable Research to Generate Effective Treatments (TARGET) portal (*https://ocg.cancer.gov/programs/target*). The fusion information and gene expression of 172 samples in our ALL cohort were obtained from the Children's Hospital of Zhejiang University School of Medicine (CNpALL).

mRNA expression analysis of partner genes in patients with fusions

Fusions were first separated into left (L) and right (R) partners. Then the $\log_2$(FC) and -$\log_{10}$(*P*_val) values were calculated by the different level of expression between patients harboring or not certain fusions using the R packages dplyr and tidyverse (code: *https://github.com/bingshaowei/ALL*).

Animal studies

Four- to six-week-old female nude mice were purchased from Ziyuan@, China. BaF3 cells were transduced with PMSCV, STK38(WT) or STK38-PXT1 lentivirus. Then, BaF3 cells (1×10^6 cells) were injected subcutaneously into the nude mice. The tumor formation rate was recorded daily. Tumors were monitored for 150 days before polymerase chain reaction (PCR)/Sanger sequencing validation. Female NSG mice (4-6 weeks old) were purchased from Nanfang Model Animal Center (China). A total of 6×10^6 transduced BaF3 cells were injected via the tail vein into the NSG mice. Peripheral blood was collected 45 days after transplantation, and the percentage of mouse CD19-positive ($mCD19^+$) cells was analyzed by flow cytometry, and overall survival was recorded. For treatment studies, venetoclax (100 mg/kg) was administered once daily by oral gavage.

Methylated RNA immunoprecipitation and quantitative polymerase chain reaction procedure

The target gene was transfected into HEK293T or BaF3 cells, and mRNA was extracted for m6A-IP using an m6A-specific antibody. The immunoprecipitation mixture, containing magnetic beads, RNase inhibitor, mRNA, IP buffer, and antibody, was incubated at 4°C for 4 hours, washed, and eluted. The purified mRNA was then quantified by quantitative polymerase chain reaction (qPCR) using the primers listed in *Online Supplementary Table S1*.

Drug screening of Food and Drug Administration-approved antitumor drugs in the BaF3 cells

PAX5-ETV6 and STK38-PXT1 BaF3 cells were treated with Food and Drug Administration (FDA)-approved drugs at clinical concentrations for 72 hours, with viability measured by CellTiter-Glo 2.0 (Promega, Beijing, China).

Statistical analysis and reproducibility

All the data are presented as the mean ± standard deviation. The statistical significance of differences between groups was determined by unpaired two-tailed Student *t* test analysis, one-way analysis of variance (ANOVA) with Tukey tests or two-way ANOVA. *P* values >0.05 are considered not statistically significant; other *P* values are denoted as follows $^*P<0.05$, $^{**}P<0.01$, $^{***}P<0.001$, $^{\#}P<0.05$, $^{\#\#}P<0.01$, $^{\#\#\#}P<0.001$.

Ethical approval

Written informed consent from patients and approval from the Institutional Research Ethics Committee of the hospital were obtained before the use of these clinical materials for research purposes. The Animal Research Committee at Zhejiang University approved all animal studies and animal care was provided in accordance with institutional guidelines. All methods were performed in accordance with relevant guidelines and regulations, including the Declaration of Helsinki.

Additional methods

Further details of the methods are provided in the *Online Supplementary Methods*.

Results

Chromosome rearrangement-enhanced mRNA stability contributes to the carcinogenic activity of classical oncofusion genes

We introduced two ALL RNA-sequencing datasets: the TARGET ALL database (679 samples from cases of high-risk B-cell ALL/acute leukemia of ambiguous lineage) and our CNpALL cohort from China Children's Hospital (172 pediatric B-cell ALL patients) (Figure 1A). We identified a total of 1,318 fusions (29 classical and 1,289 unknown fusions) in TARGET ALL and CNpALL (Figure 1B). The frequency of classical fusions was different between the TARGET ALL database and our ALL cohort which may be due to differences in patient population coverage, as the TARGET ALL did not encompass the entire spectrum of ALL samples (Figure 1C). The fusion characteristics of our ALL cohort are consistent with those of the reported primary ALL sample set.[11] We then compared the mRNA levels of partner genes in samples carrying oncofusions with those in all samples to evaluate the potential role of mRNA regulation in fusions. As shown in Figure 1D, among 29 classical fusions, the obvious mRNA level upregulation of the partner gene was found in 25 classical fusions, including eight fusions with upregulation of both left and right partner genes (Cluster I), three fusions with only left partner genes upregulated (Cluster II), and 14 fusions with only right partner genes upregulated (Cluster III). Among them, the high expression of *P2RY8* in P2RY8-IGH was reported in the literature,[21] and the high expression of *CRLF2* in P2RY8-CRLF2 resulted from promoter exchange.[12] These results suggest that mRNA upregulation may be an important regulator of the oncogenicity of gene fusions.

Next, we further analyzed the expression of L and R genes in patients without the corresponding fusion. Results showed that the upregulation of partner R in classical fusions was highly positively correlated with the L/R ratio (R^2=0.6705), whereas that of partner L was not (R^2=0.0545) (Figure 1E). These results demonstrate that the mRNA upregulation of partner R in classical fusions is primarily a consequence of promoter exchange, whereas the increased mRNA level of partner L may be attributed to alternative regulatory mechanisms. Numerous studies have highlighted the crucial role of mRNA stability in the regulation of gene mRNA levels.[22] We then used actinomycin D to inhibit mRNA synthesis and determined the mRNA degradation rate of fusions. As shown in Figure 1F and *Online Supplementary Figure S1A*, the mRNA half-life of *PAX5-ETV6* was significantly longer than that of *PAX5(WT)* both in pro-B BaF3 and HEK293T cells. Similarly, another classical fusion in Cluster I (*TCF3-PBX1*) also exhibited a markedly longer mRNA half-life compared with that of *TCF3(WT)* (Figure 1G). These results indicate that the enhanced mRNA stability may contribute to the increased partner L expression of classical fusions, thereby improving the carcinogenic activity of oncofusions.

A novel STK38-PXT1 oncofusion is identified in acute lymphoblastic leukemia based on mRNA upregulation

Besides classical oncogenic fusions, we also identified various functionally unknown fusions (Figure 1B). It is worth noting that among patients with fusions, 67.37% and 43.02% of patients had unknown fusions in TARGET and CNpALL, which were mutually exclusive with classical oncogenic drivers. We, therefore, also calculated the fold change in mRNA levels of partner genes in unknown fusion-carrying samples compared to no corresponding fusion-carrying samples. As shown in Figure 2A, B, among the 1,318 fusion genes, left partner genes (partner L) of 131 fusions and right partner genes (partner R) of 168 fusions showed enhanced mRNA levels, whereas there was only one fusion with decreased mRNA levels of a partner gene. Among them, 43 fusions (Cluster I) showed mRNA upregulation of both left and right partner genes, 88 fusions (Cluster II) exhibited only enhanced mRNA levels of left partner genes, and 125 fusions (Cluster III) displayed only increased mRNA levels of right partner genes (Figure 2C, *Online Supplementary Figure S2*).

Since chromosome rearrangement-enhanced mRNA stability may contribute to carcinogenic activity of fusions, we speculated that we could search for novel oncogenic fusions based on the phenomenon of increased mRNA stability. Based on the possibility that mRNA upregulation of partner L in fusions may result from mRNA stability regulation, we first analyzed the unknown fusions with increased mRNA levels of partner L. As shown in Figure 2D, with the annotations about whether the fusion was detected in other databases, including ChimerSeq, TCGA_StarF2019, Mitelman, ChimerKB, ChimerPub and so on, we listed the top ten recurrent fusions. Notably, increased mRNA level of *STK38* was found in ALL compared with normal bone marrow, and it was further enhanced in patients with unknown fusion STK38-PXT1 (Figure 3A). STK38 kinase, which functions in DNA damage repair, cell cycle and apoptosis, is reported to be closely associated with the development of tumors.[23]

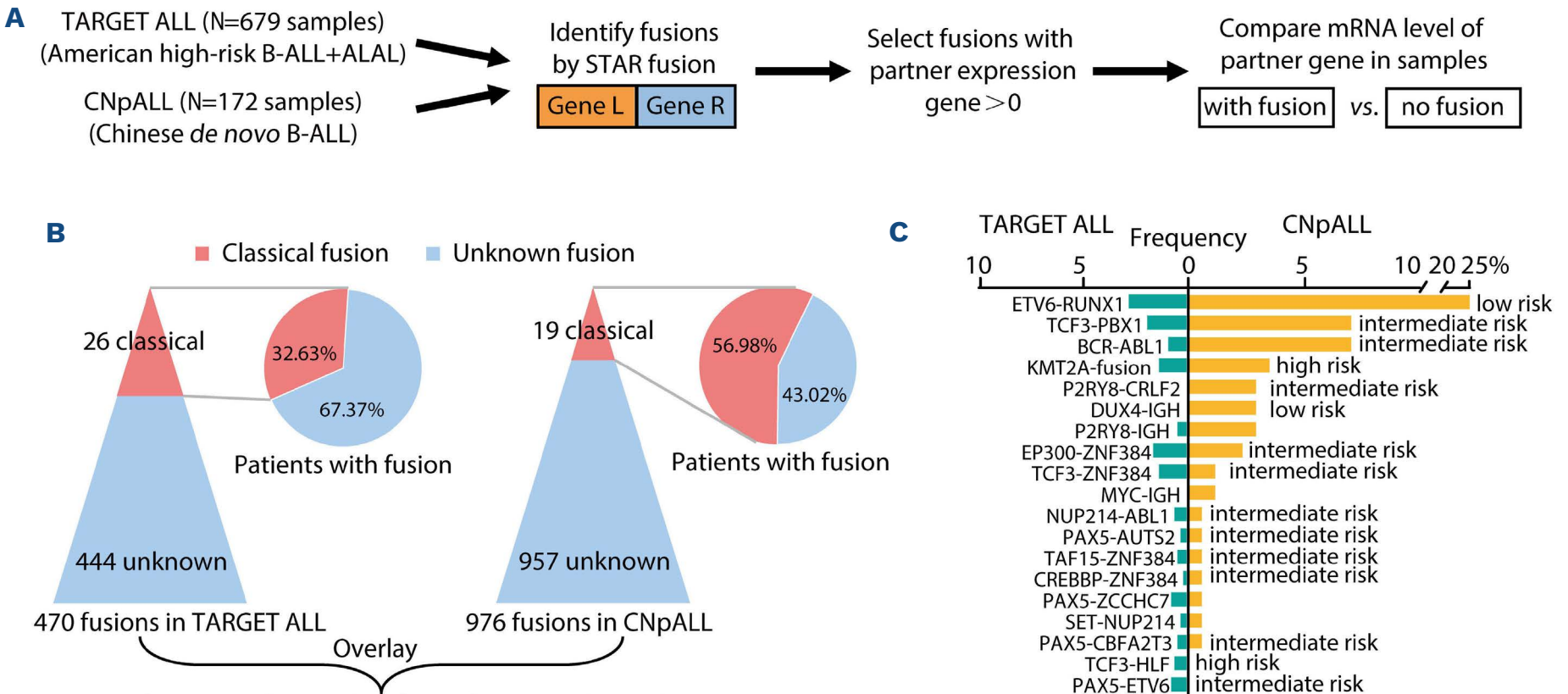


Figure 1. Chromosome rearrangement-enhanced mRNA stability contributes to carcinogenic activity of classical oncofusion genes. (A) Schematic diagram of the sample information, fusion identification and analysis process. (B) The fusion information from 679 acute lymphoblastic leukemia (ALL) samples in the TARGET ALL (Therapeutically Applicable Research to Generate Effective Treatments) database and 172 primary samples from a clinical pediatric leukemia sample cohort at the Children's Hospital of Zhejiang University School of Medicine (CNpALL). The fusion genes in samples were identified by STAR-Fusion based on whole-transcriptome sequencing.

Continued on following page.

(C) Difference in the frequency of classical oncofusions between the TARGET ALL database and our Chinese CNpALL cohort. (D) The mRNA expression of partner genes (partner L and R) in patients with classical fusions and without the corresponding oncofusion. Red: Cluster I, fusions with mRNA upregulation of both L and R partner genes. Yellow: Cluster II, fusions with only enhanced mRNA levels of L partner genes. Blue: Cluster III, fusions with only increased mRNA levels of R partner genes. Gray: Cluster IV, fusions without increased mRNA levels of L or R partner genes. (E) The correlation analysis between partner mRNA upregulation in fusions and the expression of wild-type (WT) gene. The fold change (FC) (fusion/no fusion) was calculated by comparing the mRNA level of the partner gene in samples with fusion and that in other samples. The FC(Gene L/R) was calculated by comparing the mRNA levels of the partner genes in samples without fusions. (F) The mRNA half-life ($t_{1/2}$) of *PAX5(WT)* and *PAX5-ETV6*. Genes were overexpressed in BaF3 cells, and mRNA synthesis was inhibited with actinomycin D (5 μg/mL). Samples were collected to extract mRNA at the indicated times after treatment with actinomycin. The $t_{1/2}$ was calculated by simple linear regression. (G) The mRNA $t_{1/2}$ of *TCF3(WT)* and *TCF3-PBX1*. (F, G) Data are represented as mean ± standard deviation (N=3). The significance analysis was conducted by two-way analysis of variance. **P*<0.05, ***P*<0.01 *vs.* indicated. NS: not statistically significant; B-ALL: B-cell acute lymphoblastic leukemia; ALAL: acute leukemia of ambiguous lineage; FPKM: fragments per kilobase of transcript per million mapped reads.

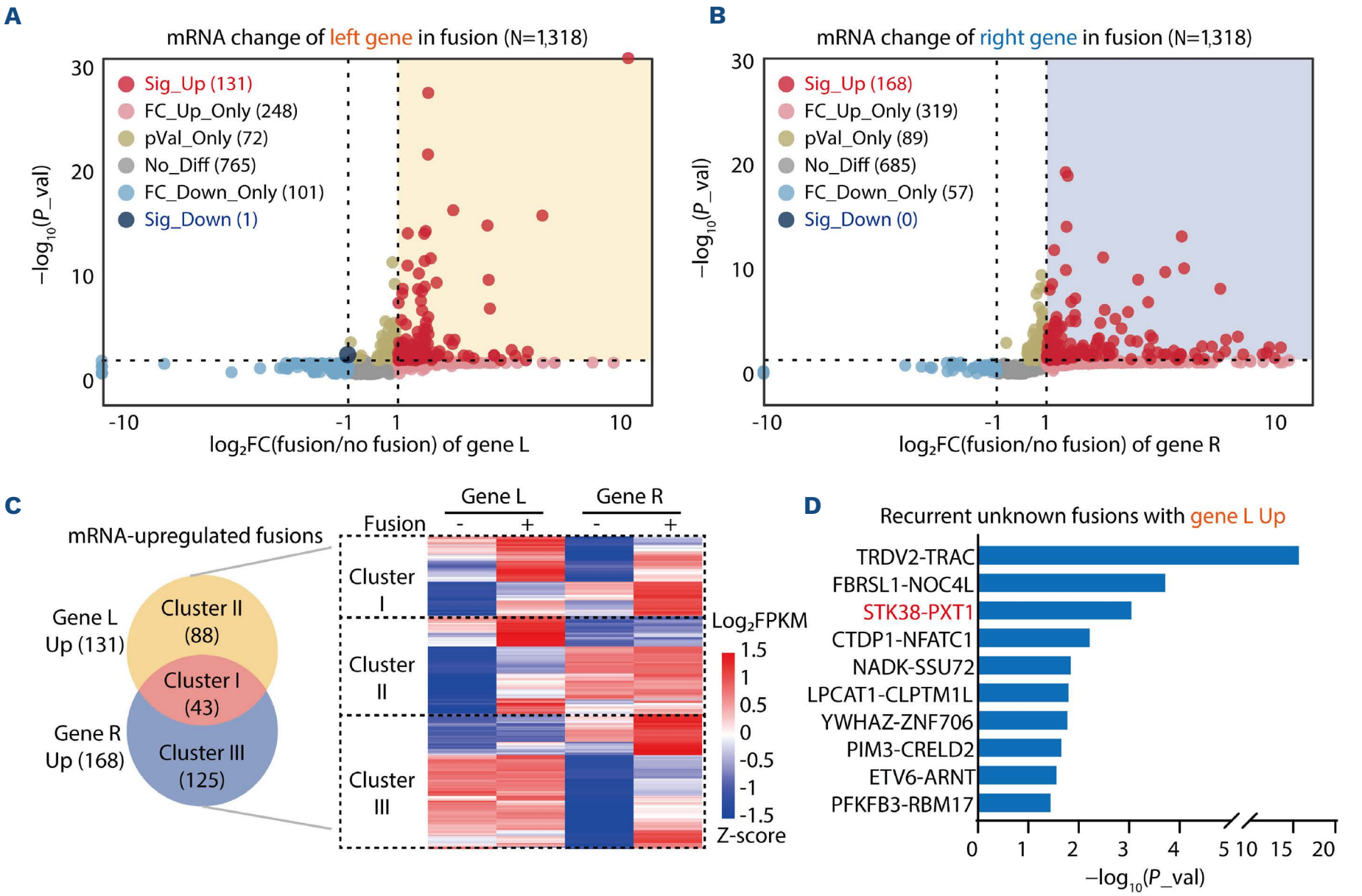


Figure 2. The prediction of potential oncofusions based on increased mRNA level of left partner genes. (A, B) mRNA level analysis of partner genes in acute lymphoblastic leukemia with classical and unknown fusions. The fold change (FC) was calculated by comparing the mRNA level of partner genes in samples with fusions and that in other samples without the corresponding fusion. The *P* value (*P*_val) was calculated by a two-tailed unpaired Student t test between samples with fusions and all samples. (A) The mRNA expression of left (L) partner genes in patients with fusions. (B) The mRNA expression of right (R) partner genes in patients with fusions. (C) The 256 fusions with significant mRNA regulation of partner genes. Red: Cluster I, fusions with mRNA upregulation of both L and R partner genes. Yellow: Cluster II, fusions with only enhanced mRNA levels of L partner genes. Blue: Cluster III, fusions with only increased mRNA levels of R partner genes. (D) The top ten recurrent unknown fusions with increased mRNA level of L partner genes. The recurrent fusions were identified through database comparison, including ChimerSeq, TCGA_StarF2019, Mitelman, ChimerKB, ChimerDB_PubMed, ChimerPub and other databases.

Moreover, we found the mRNA level of *STK38* was highest in ALL among 17 cancer types (Figure 3B). We, therefore, wondered whether STK38-PXT1 could directly drive the occurrence of ALL due to hyper-activation of STK38.

To verify this hypothesis, we first confirmed the presence of the STK38-PXT1 fusion in the patient by reverse transcriptase PCR (RT-PCR) analysis and Sanger sequencing (Figure 3C). We then demonstrated that the mRNA half-life

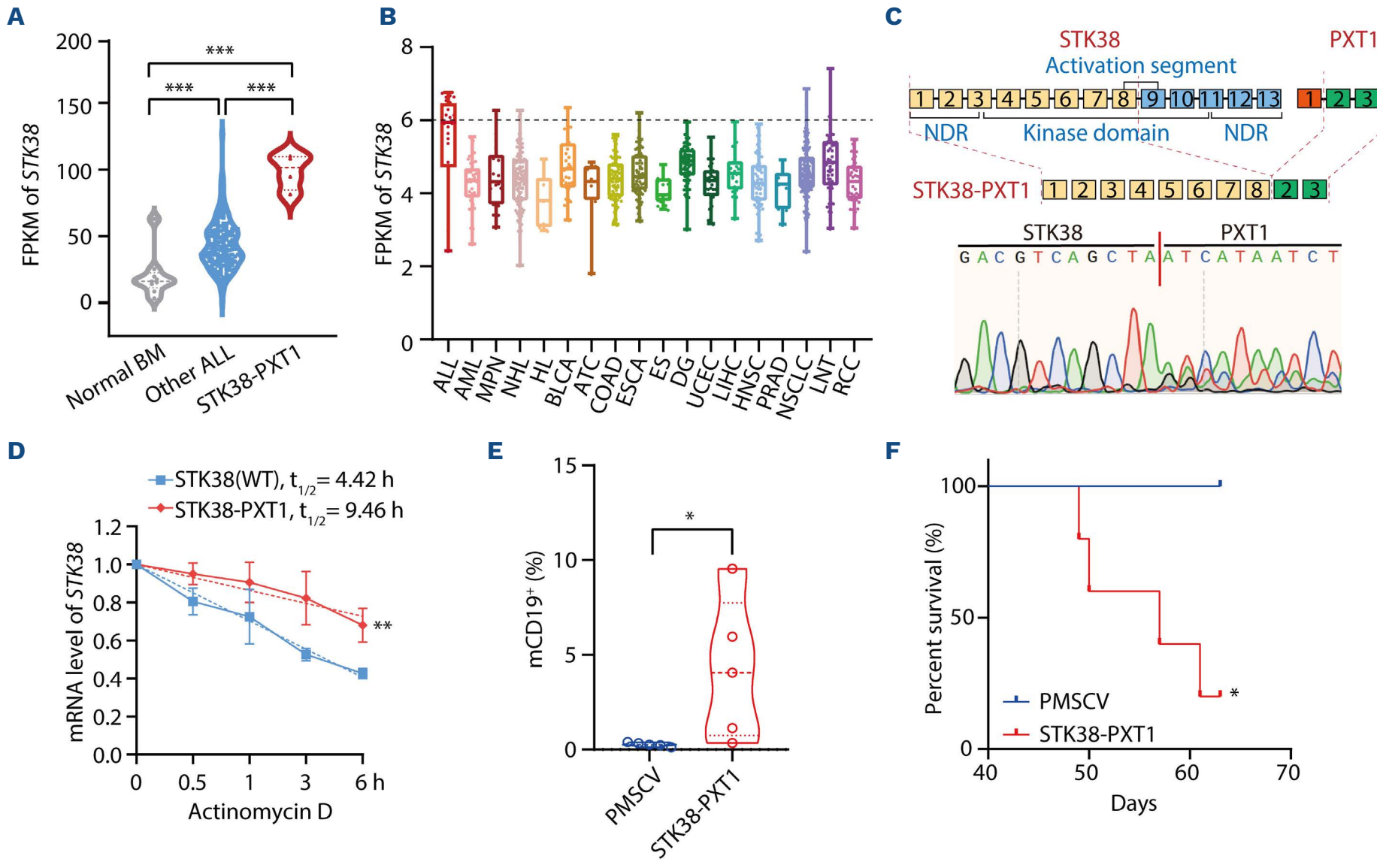


Figure 3. A novel STK38-PXT1 oncofusion identified in acute lymphoblastic leukemia based on mRNA upregulation. (A) The mRNA expression levels of the *STK38* gene in three different sample groups. Normal BM: healthy bone marrow samples collected by us; Other ALL: acute lymphoblastic leukemia samples without STK38-PXT1 in our clinical pediatric leukemia sample cohort at the Children's Hospital of Zhejiang University School of Medicine (CNpALL); STK38-PXT1: four samples specifically carrying the STK38-PXT1 fusion in our CNpALL cohort. (B) The mRNA expression levels of the *STK38* gene in different types of cancer cell lines from the Cancer Cell Line Encyclopedia (CCLE) database. (C) Schematic diagrams of wild-type STK38 protein, wild-type PXT1 protein, and STK38-PXT1 fusion protein. (D) The mRNA half-life of *STK38(WT)* and *STK38-PXT1* in BaF3 cells. Data are represented as mean ± standard deviation (N=3). (E) Percentage of mCD19$^+$ cells in peripheral blood of NSG mice 45 days after intravenous transplantation of BaF3 cells transduced with PMSCV control or *STK38-PXT1* lentivirus (N=5). (F) Kaplan-Meier overall survival curves of NSG mice transplanted with BaF3 cells expressing PMSCV control or *STK38-PXT1* (N=5). (A, D-F) The significance analysis was conducted using one-way analysis of variance (ANOVA), two-way ANOVA, an unpaired Student *t* test, or log rank test, **P*<0.05; ***P*<0.01; ****P*<0.001 *vs*. indicated. FPKM: fragments per kilobase of transcript per million mapped reads; BM: bone marrow; ALL: acute lymphoblastic leukemia; AML: acute myeloid leukemia; MPN: myeloproliferative neoplasm; NHL: non-Hodgkin lymphoma; HL: Hodgkin lymphoma; BLCA: bladder carcinoma; ATC: anaplastic thyroid cancer; COAD: colorectal adenocarcinoma; ESCA: esophageal squamous cell carcinoma; ES: Ewing sarcoma; DG: diffuse glioma; UCEC: uterine corpus endometrial carcinoma; LIHC: liver hepatocellular carcinoma; HNSC: head and neck squamous cell carcinoma; PRAD: prostate adenocarcinoma; NSCLC: non-small cell lung cancer; LNT: lung neuroendocrine tumor; RCC: renal cell carcinoma.

of *STK38-PXT1* was significantly longer than that of *STK38(WT)* both in BaF3 and HEK293T cells (Figure 3D, *Online Supplementary Figure S1B*). To further investigate the oncogenic transformation activity of the STK38-PXT1 fusion, we subcutaneously injected BaF3 cells transduced with vector-PMSCV virus, STK38(WT) and STK38-PXT1. As shown in *Online Supplementary Figure S2A*, tumors were detected only in nude mice injected with STK38-PXT1-overexpressing BaF3 cells, while no tumor was observed in mice injected with STK38(WT) or PMSCV-transduced cells. Notably, we detected the presence of the STK38-PXT1 fusion in transplanted tumors using RT-PCR analysis and Sanger sequencing (*Online Supplementary Figure S2B*). Furthermore, we designed a bone marrow transplantation model to further examine whether the STK38-PXT1 fusion can promote leukemogenesis. As shown in Figure 3E, the proportion of mCD19$^+$ cells in peripheral blood was markedly higher in the STK38-PXT1 group than in the PMSCV control group. Meanwhile, mice injected with STK38-PXT1-overexpressing BaF3 cells exhibited significantly shortened survival (Figure 3F). Together, this is the first identification of a novel fusion gene, *STK38-PXT1*, which may drive oncogenic transformation in ALL.

The STK38-PXT1 fusion drives leukemogenesis through β-catenin signaling activation

To study the carcinogenic process of STK38-PXT1, we first evaluated its effect on the proliferation and colony formation of ALL cell lines (NALM-6 and REH) as well as the pro-B BaF3 cell line. Results showed that STK38-PXT1 obviously promoted the proliferation and colony-forming capacity of NALM-6 and REH cells (Figure 4A, B, *Online Supplementary Figure S3A, B*). Additionally, STK38(WT) overexpression also promoted cell proliferation. Combined with *in vivo* carcinogenic transformation results, we suspect that STK38 kinase itself may play a tumor-promoting effect in ALL, and the STK38-PXT1 fusion can drive the leukemogenesis directly. Next, we performed differential gene analyses in BaF3 cells transfected with PMSCV, STK38(WT) and STK38-PXT1. As shown in Figure 4C, compared with PMSCV, STK38-PXT1 and STK38(WT) commonly upregulated 1,321 genes and downregulated 1,702 genes (Cluster II). STK38-PXT1 specifically upregulated 1,855 and downregulated 1,030 genes (Cluster III), while STK38(WT) specifically upregulated 1,715 and downregulated 1,207 genes (Cluster I). In Cluster II, we identified various proliferation-associated genes, which may account for the ability of both STK38(WT) and STK38-PXT1 to promote cell proliferation *in vitro* (Figure 4D, left). We also observed a large number of genes specifically upregulated only in STK38-PXT1 (Cluster III), which may be key drivers of the oncogenicity of STK38-PXT1 (Figure 4D, right). Meanwhile, STK38-PXT1 obviously promoted the proliferation and clonogenesis capacity of BaF3 cells, while the kinase mutant STK38-PXT1(K118R) did not (Figure 4E, *Online Supplementary Figure S4A, B*). We, therefore, analyzed the differential·pathway of·STK38-PXT1 and STK38(WT) as well as their K118R mutants. As displayed in Figure 4F, gene set variation analysis in hallmark pathways demonstrated that various cancer-related pathways were activated by STK38-PXT1, such as WNT_BETA_CATENIN_SIGNALING, NOTCH_ SIGNALING, and KRAS_ SIGNALING_UP, but not by STK38-PXT1(K118R) indicating that the kinase activity of STK38 may be associated with the tumorigenic effects of the fusion. Furthermore, enrichment of WNT_BETA_CATENIN_SIGNALING was also observed in STK38-PXT1 fusion-carrying leukemia samples compared with other ALL samples (Figure 4G). We, therefore, suspected that the STK38-PXT1 fusion might drive leukemogenesis by activating Wnt-β-catenin signaling.

Given that phosphorylation of GSK3β at Ser9 facilitates the transcriptional activation of β-catenin,[24] we assessed the effect of STK38-PXT1 on GSK3β phosphorylation. Results showed that the level of p-GSK3β (Ser9) was markedly increased in STK38-PXT1-overexpressing cells compared to STK38-overexpressing cells (*Online Supplementary Figure S4C*), suggesting that the increased p-GSK3β (Ser9) might contribute to the activation of β-catenin signaling in the STK38-PXT1-positive ALL cells. To further investigate the potential mechanism, we performed proteomic analyses to characterize the binding proteins of STK38-PXT1 *versus* STK38(WT). The results showed that STK38-PXT1 exhibited increased association with several proteins, with the top five being RPS18, GNB2L1, RPS25, HNRNPD and AGL (*Online Supplementary Figure S4D, E*). Among them, GNB2L1 (also known as RACK1) is reported to bind and stabilize PKC,[25,26] which has been reported to promote GSK3β phosphorylation at Ser9.[27] Based on this, we hypothesize that enhanced interactions with proteins such as RACK1 may contribute to increased GSK3β (Ser9) phosphorylation and activation of β-catenin signaling during STK38-PXT1-induced leukemogenesis.

The mRNA stability upregulation of fusions is attributable to enhanced m6A modification due to gene truncation and partner collaboration

To further investigate the molecular mechanism underlying the mRNA stability upregulation of fusions, we chose the classical fusion *PAX5-ETV6* and the newly identified fusion *STK38-PXT1* as the research subjects. Given that the generation of a fusion involves two steps, gene truncation due to chromosomal breakage and partner collaboration due to aberrant chromosomal recombination (Figure 5A), we first determined the mRNA level of partner genes in fusions containing left or right genes. For PAX5-ETV6, we analyzed the mRNA level in the different fusion genes with *PAX5* or *ETV6* from a pan-cancer database (*Online Supplementary Figure S5A*). Results showed that, as for PAX5-ETV6, the expression of *PAX5* gene was significantly upregulated in all other PAX5 fusions, whereas the level of *ETV6* fusion partners was unchanged (Figure 5B), indicating that the gene truncation may contribute to the increased mRNA level in PAX5 fusions. Meanwhile, no significant change of *STK38* expression was observed in other STK38 fusions, whereas the level of the *PXT1* fusion partner was upregulated in different PXT1 fusions (Figure 5C, *Online Supplementary Figure S5B*), suggesting that the PXT1 partner may help to enhance the mRNA level of partners such as *STK38*. To further investigate the role of gene truncation and partner collaboration in the increased mRNA stability of *PAX5-ETV6* and *STK38-PXT1* fusions, we introduced PAX5(N) and STK38(N), which represent the N-terminal fragments of PAX5 in the PAX5-ETV6 fusion and STK38 in the STK38-PXT1 fusion, respectively. As shown in Figure 5D and *Online Supplementary Figure S5C*, the mRNA half-life of *PAX5-ETV6* as well as *PAX5(N)* was significantly longer than that of *PAX5(WT)* both in BaF3 and HEK293T cells. For STK38-PXT1, the mRNA half-life of *STK38-PXT1* was significantly longer than that of *STK38(WT)*, while that of *STK38(N)* was not (Figure 5E, *Online Supplementary Figure S5D*). Collectively, these findings indicate that gene truncation and partner collaboration may regulate the mRNA stability of *PAX5* fusion and *STK38-PXT1*.

Given that m6A modification is an important way to modulate mRNA stability, we compared the m6A modification level of the fusion gene and the truncated gene by methylated RNA immunoprecipitation (MeRIP) assay (*Online Sup-*

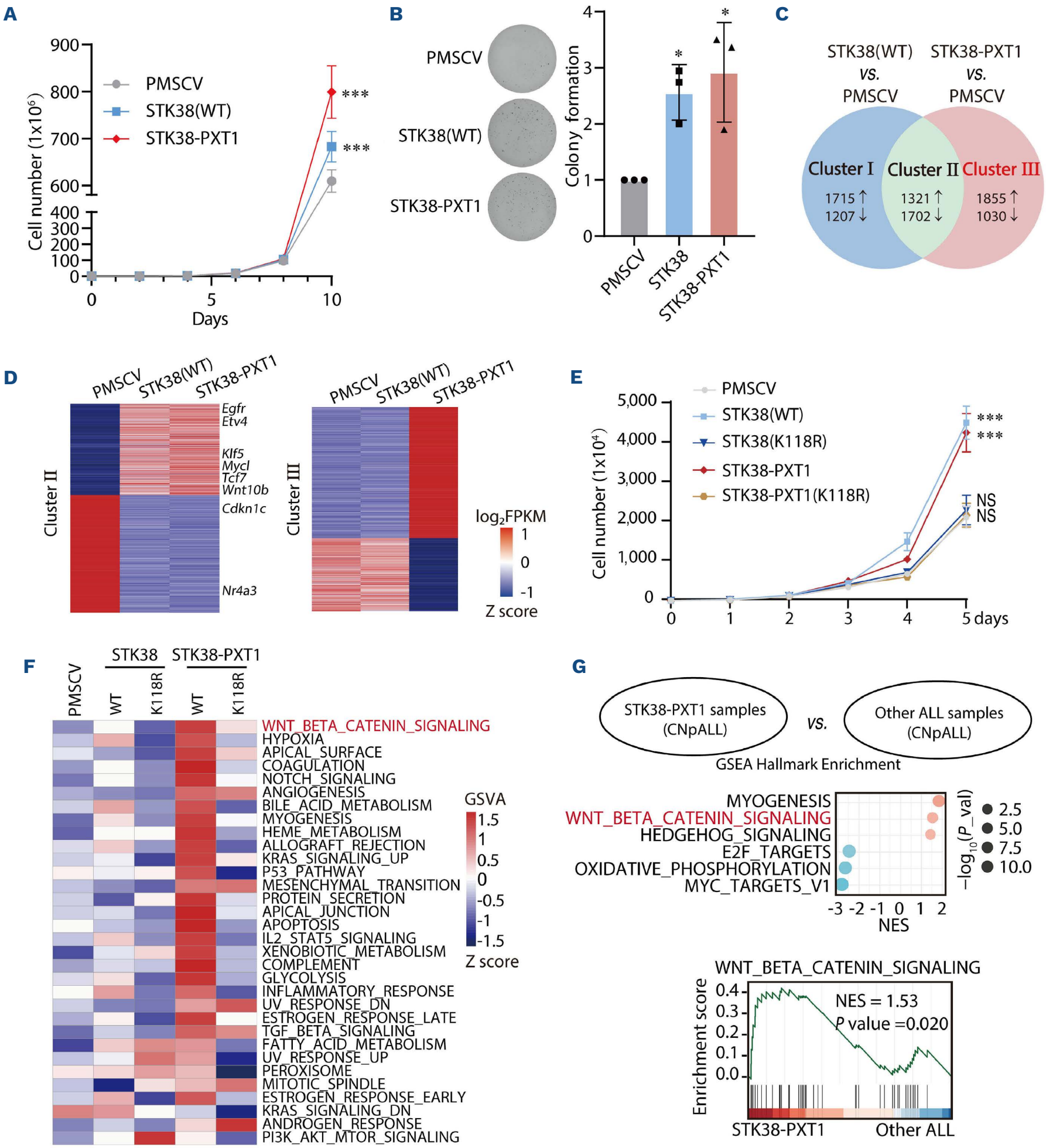


Figure 4. The STK38-PXT1 fusion drives leukemogenesis through β-catenin signaling activation. (A) Proliferation curve of NALM-6 cells overexpressing STK38-PXT1 and STK38(WT). (B) The colony-forming ability of NALM-6 cells overexpressing STK38(WT), and STK38-PXT1. (C, D) Venn diagram (C) and heatmap (D) of differential gene analysis between STK38-PXT1 and STK38(WT). The differential gene analysis was performed by comparing the gene expression profiles in BaF3 cells transfected with STK38-PXT1 and vector-PMSCV, or BaF3 cells transfected with STK38(WT) and vector-PMSCV. (C) The Venn diagram shows differential gene analysis between STK38-PXT1 and STK38(WT). Cluster I: only changed in STK38(WT); Cluster II: changed in both STK38(WT) and STK38-PXT1; Cluster III: only changed in STK38-PXT1. (D) Genes from Clusters II (Left) and III (Right). Genes related to cell proliferation in Cluster II are indicated in the heatmap. (E) Proliferation curve of BaF3 cells overexpressing STK38-PXT1. BaF3 cells

Continued on following page.

were transfected with lentivirus PMSCV, STK38(WT), STK38(K118R), STK38-PXT1, and STK38-PXT1(K118R). (F) Gene set variation analysis hallmark enrichment across PMSCV, STK38(WT), STK38(K118R), STK38-PXT1, and STK38-PXT1(K118R). (G) Top: gene set enrichment analysis (GSEA) hallmark enrichment between samples with STK38-PXT1 and other acute lymphoblastic leukemia (ALL) samples in our CNpALL cohort. Bottom: GSEA plots depicting enrichment of Wnt-β-catenin signaling in the transcriptional profiling of samples with STK38-PXT1 and other ALL samples in our ALL cohort. (A, B, E) Data are represented as mean ± standard deviation (N=3). The significance analysis was conducted using one-way or two-way analysis of variance. NS=*P*>0.05; **P*<0.05; ****P*<0.001 *vs*. PMSCV. WT: wild-type; FPKM: fragments per kilobase of transcript per million mapped reads; GSVA: gene set variation analysis; CNpALL: clinical pediatric leukemia sample cohort at the Children's Hospital of Zhejiang University School of Medicine; NES: normalized enrichment score.

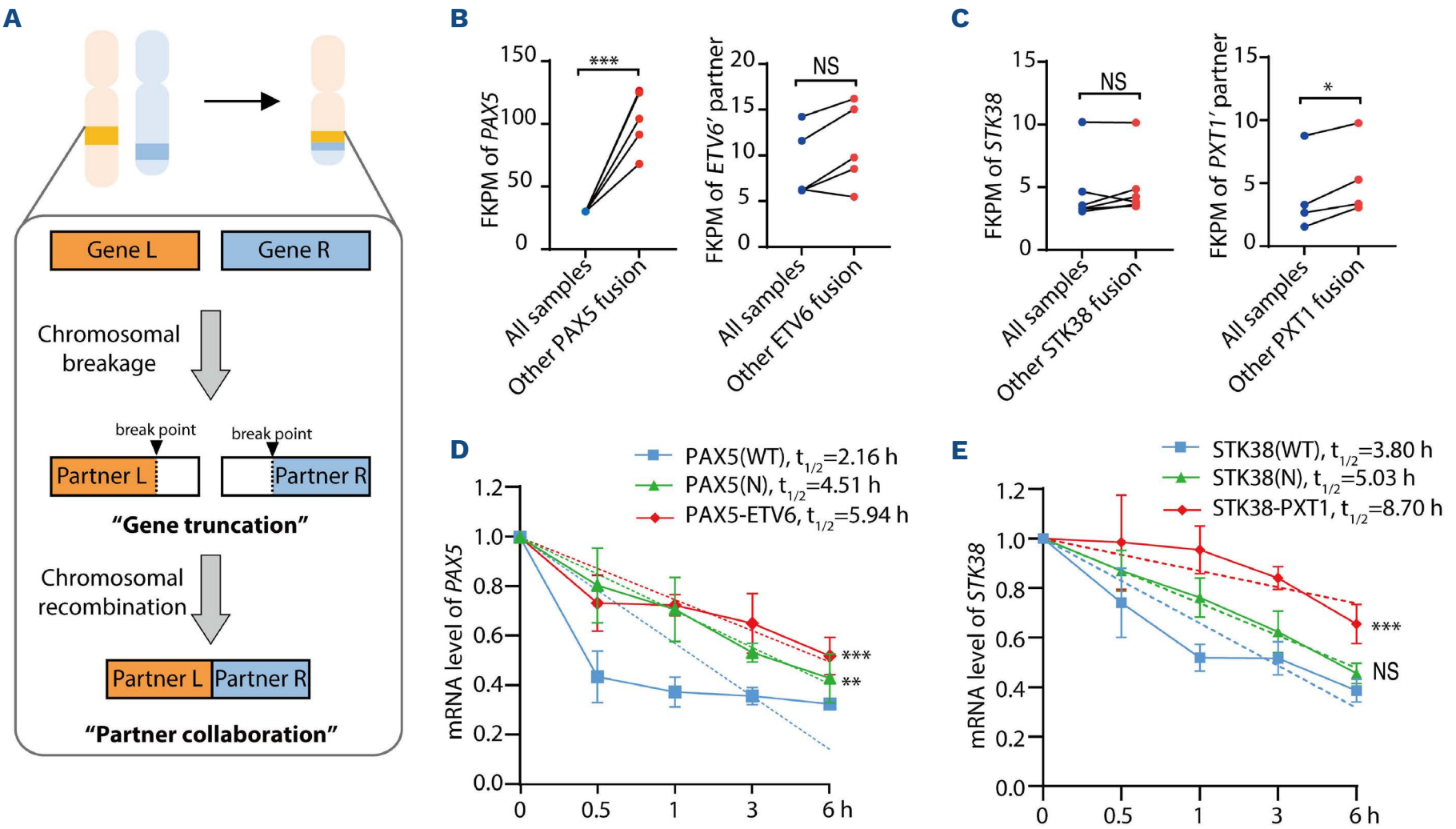


Figure 5. Gene truncation and partner collaboration regulate the mRNA stability of PAX5 fusion and STK38-PXT1. (A) Schematic generation of fusions involving gene truncation and partner collaboration. (B) Left: FPKM (fragments per kilobase of transcript per million mapped reads) level of the *PAX5* gene in five *PAX5* fusion genes excluding PAX5-ETV6 in the TARGET ALL database. Right: FPKM level of the 5'-terminal genes of five other ETV6 fusion genes except PAX5-ETV6 in The Cancer Genome Atlas (TCGA) database. (C) Left: FPKM level of the *STK38* gene in six STK38 fusion genes excluding STK38-PXT1 in the TCGA database. Right: FPKM level of 5'-terminal genes of another five PXT1 fusion genes except STK38-PXT1 in the TCGA database. (D) mRNA half-life of *PAX5(WT)*, *PAX5(N)* and *PAX5-ETV6* in BaF3 cells. (E) mRNA half-life of *STK38(WT)*, *STK38(N)* and *STK38-PXT1* in BaF3 cells. (D, E) Data are represented as mean ± standard deviation (N=3). (B-E) The significance analysis was conducted using a two-tailed unpaired Student *t* test, two-way analysis of variance. NS=*P*>0.05; **P*<0.05; ***P*<0.05; ****P*<0.001 *vs*. indicated. L: left; R: right; WT: wild-type, $t_{1/2}$: half-life.

plementary Figure S5E). The results showed that the m6A modification level of *PAX5-ETV6* and *PAX5(N)* was higher than that of *PAX5(WT)* in BaF3 and HEK293T cells (Figure 6A, *Online Supplementary Figure S5F*). Meanwhile, the m6A modification level of *STK38-PXT1* was higher than that of *STK38(WT)* and *STK38(N)* (Figure 6B, *Online Supplementary Figure S5G*). These results were highly consistent with the mRNA stability changes observed in PAX5-ETV6 and STK38-PXT1. Thus, we further analyzed the potential m6A modification sites within *PAX5-ETV6* and *STK38-PXT1*. We first used the m6A prediction tool SRAMP to identify putative methylation sites within both *PAX5-ETV6* and *STK38-PXT1* fusions, and then we generated point mutant constructs at predicted adenines to find the potential m6A sites. For *PAX5-ETV6*, predicted potential methylation sites were A43 and A48 in the *PAX5* segment and A614, A843, A1322 and A1437 in the *ETV6* segment (*Online Supplementary Table S3*). Given the comparable m6A levels between *PAX5(WT)* and *PAX5(N)*, we hypothesized that the functional m6A sites may be located on the *PAX5* segment. mRNA stabili-

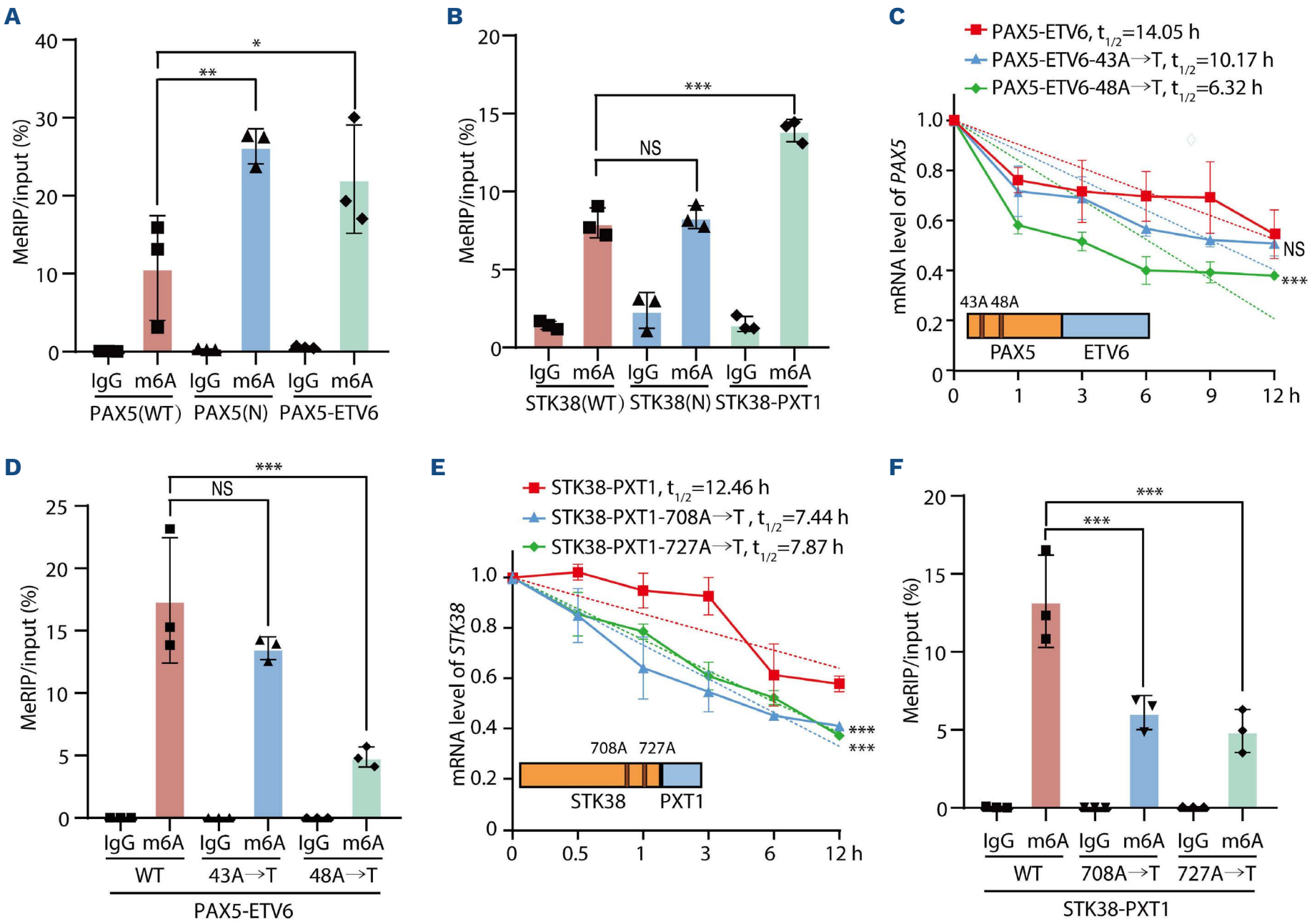


Figure 6. The mRNA stability upregulation of fusions is attributed to enhanced m6A modification. (A) The m6A modification level of *PAX5(WT)*, *PAX5(N)* and *PAX5-ETV6* in BaF3 cells. (B) The m6A modification level of *STK38(WT)*, *STK38(N)* and *STK38-PXT1* in BaF3 cells. (C) mRNA half-life of *PAX5-ETV6(WT)*, *PAX5-ETV6(43A→T)*, and *PAX5-ETV6(48A→T)* in HEK293T cells. (D) The m6A modification level of *PAX5-ETV6(WT)*, *PAX5-ETV6(43A→T)*, and *PAX5-ETV6(48A→T)* in HEK293T cells. (E) mRNA half-life of *STK38-PXT1(WT)*, *STK38-PXT1 (708A→T)*, and *STK38-PXT1 (727A→T)* in HEK293T cells. (F) The m6A modification level of *STK38-PXT1(WT)*, *STK38-PXT1 (708A→T)*, and *STK38-PXT1 (727A→T)* in HEK293T cells. (A-F) Data are represented as mean ± standard deviation (N=3). The significance analysis was conducted using a two-tailed paired Student *t* test, one-way or two-way analysis of variance. NS=*P*>0.05; **P*<0.05; ***P*<0.01; ****P*<0.001 *vs*. indicated. MeRIP: methylated RNA immunoprecipitation.

ty assays and MeRIP-qPCR assay results showed that the A48T mutation markedly reduced the half-life and m6A enrichment of *PAX5* transcripts, whereas the A43T mutation did not have a no significant effect (Figure 6C, D). For *STK38-PXT1*, predicted m6A sites were located exclusively within the *STK38* segment (A545, A565, A602, A662, A681, A689, A708 and A727) (*Online Supplementary Table S4*). Based on SRAMP scores, we selected the top two sites to evaluate. The results showed that both A727T and A708T mutations significantly reduced mRNA stability and m6A modification of *STK38-PXT1* compared with the wild-type *STK38* (Figure 6E, F). Taken together, these results suggest that enhanced m6A modification due to gene truncation and partner collaboration may contribute to the enhanced mRNA stability of fusions.

The m6A reader IGF2BP3 is responsible for maintaining the high stability of fusion mRNA

The m6A modification level is regulated by m6A methyltransferases (writers) and demethylases (erasers), and its regulation of mRNA stability requires reader proteins.[16] We suspect that key m6A readers stabilizing oncofusions could be promising therapeutic targets. Thus, we first analyzed the expression of m6A modulators (writers, erasers and readers) in ALL samples carrying PAX5 fusions and STK38-PXT1 fusions. Interestingly, the m6A reader *IGF2BP3* was specifically upregulated in both PAX5 fusion and STK38-PXT1 fusion samples (Figure 7A, B, *Online Supplementary Figure S6A*) and compared with other classical oncofusions, patients carrying PAX5 fusions showed the highest level of *IGF2BP3* (Figure 7C). In addition, the *IGF2BP3* upregulation

in KMT2A fusions is consistent with the literature.[28] Furthermore, shIGF2BP3 reduced mRNA stability of *PAX5(N)* and *PAX5-ETV6* but not *PAX5(WT)* (Figure 7D), and the mRNA half-life of *STK38-PXT1* rather than *STK38(WT)* and *STK38(N)* was markedly shortened by shIGF2BP3 (Figure 7E). These results indicate that IGF2BP3 may be the crucial reader for regulating the high mRNA stability of these fusions.

Next, to identify the potential therapeutic effect of IGF2BP3 in ALL driven by fusions with high mRNA stability, we investigated the effect of silencing IGF2BP3 in the proliferation of PAX5-ETV6- and STK38-PXT1-overexpressing BaF3 cells. As shown in Figure 7F, G, we found that compared with PAX5(WT), shIgf2bp3 (#1 and #2) had a stronger inhibitory effect on cell proliferation on PAX5-ETV6 as well as PAX5(N). Similar to PAX5-ETV6, the inhibition rate of shIgf2bp3 in the STK38-PXT1-overexpressing BaF3 cells was higher than that in STK38(WT)-overexpressing BaF3 cells, while this enhanced inhibitory effect was not observed in STK38(WT)-overexpressing BaF3 cells (Figure 7H). These results suggest IGF2BP3 as a novel candidate for therapeutic intervention for patients with ALL driven by these fusions with stabilized mRNA.

Given that IGF2BP3 was elevated in PAX5 fusion and STK38-PXT1-positive ALL (*Online Supplementary Figure S6A*), we assessed whether other IGF2BP3 target genes were upregulated. Although IGF2BP3 can stabilize *c-MYC* in KMT2A-rearranged ALL,[29] *c-MYC* was not increased in our fusion-positive cells (*Online Supplementary Figure S6B*). Comparing upregulated genes in these patients with IGF2BP3 RIP-sequencing data revealed 125 overlapping candidates, including various cancer-related genes (*Online Supplementary Figure S6C, D*), which may represent potential IGF2BP3 targets in this subset of ALL. Meanwhile, we also explored potential mechanisms underlying *IGF2BP3* upregulation in these patients. We found that *BRD4*, a reported transcriptional activator of IGF2BP3,[30] was significantly elevated in both fusion-positive subtypes (*Online Supplementary Figure S6E*) and in IGF2BP3-high *versus* IGF2BP3-low ALL samples (*Online Supplementary Figure S6F*), suggesting that *BRD4* upregulation may contribute to IGF2BP3 overexpression in this context.

Venetoclax specifically inhibits mRNA high-stability fusion-driven acute lymphoblastic leukemia

Based on the above finding that shIGF2BP3 could effectively inhibit the cell proliferation-promoting ability of PAX5-ETV6 and STK38-PXT1, targeting IGF2BP3 may be the ideal strategy for treatment of these fusion-driven ALL. Due to the lack of approved IGF2BP3 inhibitors, we next searched for potential clinically accessible marketed drugs with potential efficacy against PAX5-ETV6- or STK38-PXT1-rearranged ALL. First, we evaluated the inhibition rate of 102 FDA-approved antitumor drugs in the BaF3 cells that overexpressed PAX5-ETV6 and STK38-PXT1. The results showed that the inhibition rate of venetoclax in the PAX5-ETV6 group was 30.63% higher than that in the PAX5(WT) group, ranking second among 102 antitumor drugs (Figure 8A). For STK38-PXT1, the inhibition rate of venetoclax in the STK38-PXT1 cells was 48.78% higher than that in the STK38(WT) group, ranking first among 102 antitumor drugs (Figure 8B). Additionally, we also analyzed the drug-response profiles according to *IGF2BP3* expression levels in ALL cells, and found that venetoclax cytotoxicity was significantly greater in *IGF2BP3*-high cells (Figure 8C, *Online Supplementary Figure S7A, B*). Thus, we hypothesized that venetoclax may represent a potential therapeutic agent for PAX5-ETV6- or STK38-PXT1-positive ALL.

Furthermore, we assessed the apoptosis-inducing effect of venetoclax in PAX5-ETV6- and STK38-PXT1-overexpressing cells. The results showed that compared with vector-PMSCV (22.54±1.30%) and PAX5(WT) (28.37±7.52%), the apoptosis rate of PAX5-ETV6 cells upon exposure to venetoclax was further enhanced (70.85±3.45%) (Figure 8D, *Online Supplementary Figure S7C*). Similarly, a higher rate of venetoclax-induced apoptosis was observed in STK38-PXT1 cells (57.34±3.58%) than in STK38(WT) (28.79±2.98%) and vector-PMSCV (15.71±0.59%) cells (Figure 8E, *Online Supplementary Figure S7D*). Consistently, dose-dependent apoptosis induction by venetoclax was observed in both PAX5-ETV6- and STK38-PXT1-overexpressing cells (*Online Supplementary Figure S7E*). These results indicate that venetoclax exhibited selective cellular activity-inhibitory and apoptosis-inducing effects on BaF3 cells carrying PAX5-ETV6 and STK38-PXT1.

To explore the underlying mechanism, we first assessed the expression of *BCL2* in BaF3 cells stably expressing either PAX5-ETV6 or STK38-PXT1 fusion genes. The results showed that the expression of *BCL2* as well as other apoptotic players in cases carrying PAX5 fusions or STK38-PXT1 was comparable to that in the remaining patients (*Online Supplementary Figure S8A, B*). We then performed gene set enrichment analysis comparing PAX5 fusion and STK38-PXT1 fusion-positive *versus* fusion-negative cases. We found that the OXIDATIVE_PHOSPHORYLATION (OXPHOS) pathway was significantly downregulated in both PAX5-ETV6- and STK38-PXT1-positive samples (Figure 8F, G). This is noteworthy as previous studies have shown that reduced OXPHOS activity is strongly associated with heightened venetoclax sensitivity in AML.[31-34] Considering all these findings together, we hypothesize that decreased OXPHOS activity is a key vulnerability that contributes to the enhanced venetoclax sensitivity observed in PAX5-ETV6- or STK38-PXT1-expressing cells.

Finally, we evaluated the antileukemic activity of venetoclax *in vivo* using NSG mouse xenograft models established by intravenous engraftment of BaF3 cells expressing PAX5-ETV6 or STK38-PXT1. The results showed that venetoclax significantly suppressed the expansion of circulating mCD19$^+$ cells in both leukemia models (Figure 8H) and significantly prolonged the overall survival of leukemic mice (Figure 8I),

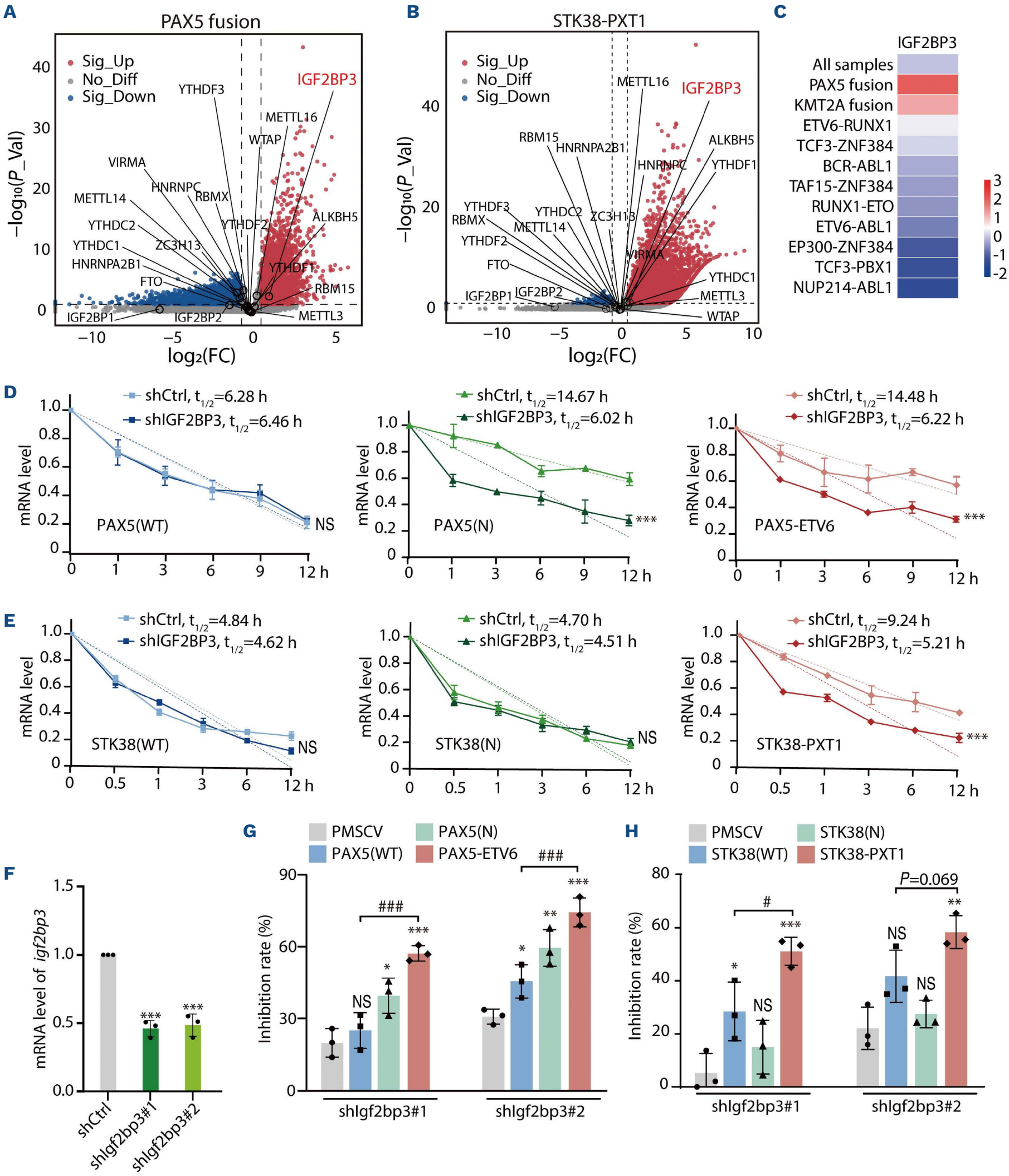
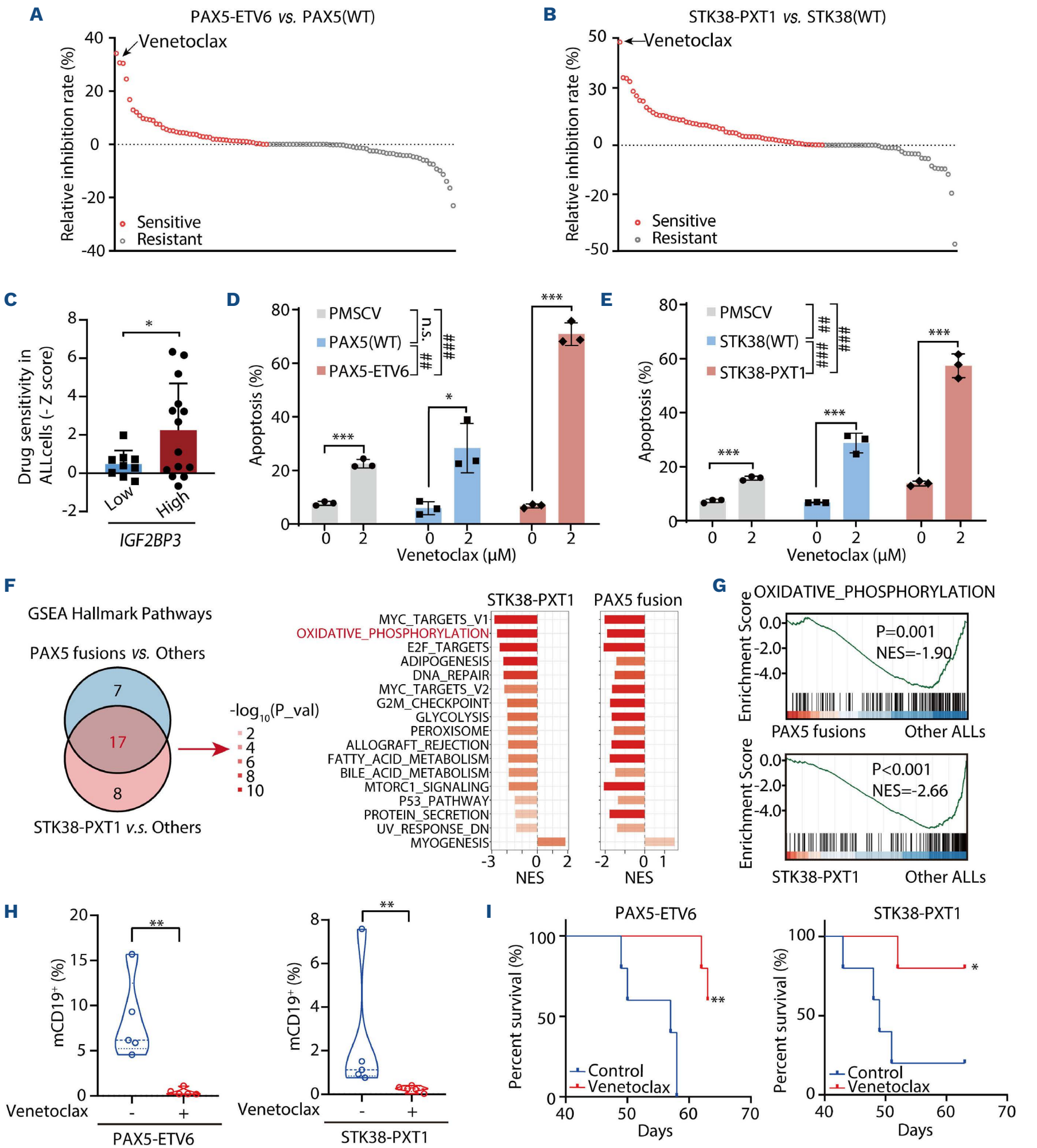


Figure 7. The m6A reader IGF2BP3 is responsible for maintaining the high stability of fusion mRNA. (A) The differentially expressed genes of acute lymphoblastic leukemia (ALL) patients with PAX5 fusions. Compared with 657 ALL samples without PAX5 fusions, the differential gene expression volcano plot of 22 ALL samples with a PAX5 fusion in the TARGET database. (B) The differentially expressed genes of ALL patients with the STK38-PXT1 fusion. Compared with 168 ALL patients, the differential gene expression

Continued on following page.

volcano plot of four patients with the STK38-PXT1 fusion in our ALL database. (C) The expression levels of *IGF2BP3* in ALL samples with different classical oncofusions. (D) The effect of shIGF2BP3 on the mRNA half-life of *PAX5(WT)*, *PAX5(N)* and *PAX5-ETV6*. (E) The effect of shIGF2BP3 on the mRNA half-life of *STK38(WT)*, *STK38(N)* and *STK38-PXT1*. (D, E) The mRNA half-life ($t_{1/2}$) was detected by an actinomycin D experiment and calculated by simple linear regression. (F) The silencing effect of shIgf2bp3 on BaF3 cells. (G) The proliferation-inhibitory effect of shIgf2bp3 on BaF3 cells overexpressing vector-PMSCV, PAX5(WT), PAX5(N) and PAX5-ETV6. (H) The proliferation-inhibitory effect of shIgf2bp3 on BaF3 cells overexpressing vector-PMSCV, STK38(WT), STK38(N) and STK38-PXT1. (D-H) Data are represented as mean ± standard deviation (N=3). The significance analysis was conducted using one-way or two-way analysis of variance. NS=*P*>0.05; **P*<0.05; ***P*<0.01; ****P*<0.001 *vs*. indicated.



Continued on following page.

Figure 8. Venetoclax specifically inhibits mRNA high-stability fusion-driven acute lymphoblastic leukemia. (A) Selective sensitivity of BaF3 cell lines overexpressing PAX5-ETV6 to antitumor drugs compared with the sensitivity of those expressing PAX5(WT). (B) Selective sensitivity of BaF3 cell lines overexpressing STK38-PXT1 to antitumor drugs compared with the sensitivity of those expressing STK38(WT). (A, B) Relative inhibition rate (%): the inhibition ratio of the indicated fusion gene group to the respective wild-type. (C) Z-score, the mean sensitivity score, of 23 acute lymphoblastic leukemia (ALL) cell lines to venetoclax. *IGF2BP3* Low: Z-score of nine cell lines with low levels of *IGF2BP3* expression, marked in black; *IGF2BP3* High: Z-score of 14 cell lines with high levels of *IGF2BP3* expression, marked in red. (D) The apoptosis rate-induced by venetoclax in the BaF3 cells overexpressing vector-PMSCV, PAX5(WT) and PAX5-ETV6. (E) The apoptosis rate induced by venetoclax in the BaF3 cells overexpressing vector-PMSCV, STK38(WT) and STK38-PXT1. (D, E) Apoptosis of cells induced by 2 μM venetoclax was investigated by flow cytometry with annexin V – propidium iodide double staining. (F) Gene set enrichment analysis (GSEA) hallmark pathway overlap in PAX5 fusion and STK38-PXT1-positive ALL. Left: Venn diagram of significantly enriched hallmark gene sets in PAX5 fusion-positive *versus* fusion-negative patients and in STK38-PXT1-positive *versus* fusion-negative patients. Right: shared hallmark pathways uniquely enriched in both fusion-positive groups, displayed with normalized enrichment scores (NES) for each comparison; color intensity reflects statistical significance ($-\log_{10}$ *P* value). (G) GSEA enrichment plots for the HALLMARK_OXIDATIVE_PHOSPHORYLATION pathway in PAX5 fusion-positive *versus* fusion-negative patients and STK38-PXT1-positive *versus* fusion-negative patients. (H, I) *In vivo* antileukemic activity of venetoclax in NSG mouse models of PAX5-ETV6- and STK38-PXT1-driven leukemia. NSG mice were intravenously engrafted with BaF3 cells overexpressing PAX5-ETV6 or STK38-PXT1, and treated with venetoclax (100 mg/kg/day by oral gavage) (N=5 per group). (H) Percentages of $mCD19^+$ cells in peripheral blood at day 45 after transplantation. (I) Kaplan-Meier curves for overall survival. (D, E) Data are represented as mean ± standard deviation (N=3). (C-E, H, I) The significance analysis was conducted using a two-tailed unpaired Student *t* test, two-way analysis of variance or log rank test. NS=*P*>0.05; **P*<0.05; ****P*<0.001 *vs*. indicated; $^{\#}P$<0.05; $^{\#\#}P$<0.01; $^{\#\#\#}P$<0.001 *vs*. indicated.

confirming its potent *in vivo* efficacy. Collectively, these results demonstrate that venetoclax exerts potent and selective antileukemic activity against PAX5-ETV6- and STK38-PXT1-driven ALL.

Discussion

Emerging evidence suggests that m6A methylation plays a critical role in cancer through various mechanisms. Alterations in m6A modification of various tumor-promoting genes such as *BRD4*, *MYC*, *SOCS2* and *EGFR* are important in cancer pathogenesis and progression.[18] Here, we first report that the m6A modification alteration is important for oncogenic fusions. Both the well-established oncogenic fusion *PAX5-ETV6* and the novel oncofusion *STK38-PXT1* show upregulated mRNA stability compared with wild-type *PAX5* and *STK38*. Interestingly, we found that the increased mRNA stability separately results from gene truncation and partner collaboration. It has been reported that exon architecture controls mRNA m6A suppression through exon junction complexes.[35] It is possible that gene truncation may lead to the loss of interaction between exon junction complexes and mRNA, followed by m6A modification upregulation. For STK38-PXT1, inclusion of PXT1 may rewire the protein-protein interaction landscape, which may be associated with increased stability of the *STK38* mRNA. Future work is needed to define how PAX5 C-terminal truncation and the PXT1 partner promote m6A modification of these fusions.

While gene fusion events in cancers have been extensively documented, their oncogenic functions remain largely unknown.[36] Currently, the approaches to identify key oncogenic fusions are mainly based on clinical information and unique transcriptional characteristics. For example, we have previously identified a novel gene fusion RUNX1-ZNF423 in a 1-year-old male patient with acute myeloid leukemia with repeated relapses and chemoresistance.[37] St. Jude Children's Research Hospital illustrated a new oncogenic subtype with DUX4 fusion that was marked by a unique paradigm of transcription factor deregulation in leukemia.[38] A study about the transcriptional landscape of B-cell ALL based on an international study of 1,223 cases identified a new ZNF362 fusion.[39] Here, combined with enhanced mRNA levels and mutual exclusivity with classical oncogenic drivers, we discovered a novel oncogenic fusion STK38-PXT1. In addition, we also identified 256 fusions, such as TRDV2-TRAC, FBRSL1-NOC4L and others, with enhanced partner mRNA levels, whose function needs further investigation.

STK38 is composed of 13 exons, with exons 1-3 encoding the N-terminal regulatory domain and exons 3-11 encoding the kinase domain.[40] The STK38-PXT1 fusion protein retains all N-terminal regulatory domains and portions of the kinase domain (exons 3-8). Our RNA-sequencing analysis indicated that activation of the β-catenin pathway may contribute to the oncogenic mechanism of STK38-PXT1. Moreover, combined with the proteomic data, we hypothesize that enhanced interactions between STK38-PXT1 and proteins such as RACK1 may contribute to increased GSK3β phosphorylation at Ser9 and the activation of β-catenin signaling during leukemogenesis. Certainly, these interactions and their relationship to β-catenin activation need further in-depth investigation.

Abnormal alterations in m6A modification have been reported to be closely associated with leukemia, especially acute myeloid leukemia. Multiple m6A modulators, such as writer METTL16,[41] erasers FTO[42,43] and ALKBH5,[44,45] and readers YTHDF1,[46] YTHDC1,[47] IGF2BP2[48] and IGF2BP3,[49] have been reported to regulate the progression of acute myeloid leukemia. Our study showed that IGF2BP3 may be the ideal target for PAX5-ETV6 or STK38-PXT1 fusion-driven ALL. Therefore, pharmacological inhibition of IGF2BP3, for example with the small-molecule inhibitor AE-848, may represent a promising treatment strategy.[50] Furthermore,

we showed that these fusion-positive ALL cells exhibit sensitivity to venetoclax. We found a marked suppression of OXPHOS in fusion-positive cases rather than *BCL2* up-regulation. It has been reported that low OXPHOS activity strongly correlates with heightened venetoclax sensitivity in leukemia.[31-34] Mechanistically, leukemic cells with intrinsically low OXPHOS rely heavily on BCL-2 to maintain mitochondrial outer membrane integrity; inhibition of BCL-2 in such cells rapidly triggers mitochondrial outer membrane permeabilization, cytochrome-c release, caspase activation, and prompt apoptosis.[31] Collectively, these findings suggest that reduced OXPHOS activity represents a metabolic vulnerability that underlies the increased venetoclax sensitivity of PAX5-ETV6- or STK38-PXT1-expressing cells.

Collectively, our findings unveil novel oncogenic mechanisms underpinned by m6A modification and mRNA stability in fusion genes. These insights not only facilitate the discovery of novel oncogenic fusions, but also pave the way for innovative strategies aimed at unraveling oncogenic fusion events.

Disclosures

No conflicts of interest to disclose.

Contributions

MY, XS and JZ conceived the study and analyzed data. MY and XS organized the figures and wrote the manuscript. JZ and DS collected the fusion and clinical information of our cohort of patients with acute lymphoblastic leukemia. XS, ZX and SB performed the fusion analysis. ZX, MC, CS, TW and WD performed the animal study and in vitro assay. XS, ZX, JL and XX collected and analyzed the RNA-sequencing data. JC, BY and QH conceived the experiments and helped to organize the paper.

Funding

This work was supported by the Zhejiang Provincial Natural Science Foundation of China (N. LY24H080002 to JZ), the Natural Science Fund for Distinguished Young Scholars of Zhejiang Province (N. LR23H310001 to MY, N. LR24H310001 to XS), and the Fundamental Research Funds for the Central Universities (N. 226-2025-00136 to MY).

Data-sharing statement

The datasets analyzed during the current study are available from the Therapeutically Applicable Research to Generate Effective Treatments (TARGET) portal (https://ocg.cancer.gov/programs/target). Raw data for RNA-sequencing are deposited at the NCBI GEO (GSE275289). Additional data related to this subject are available from the corresponding author on reasonable request.

References

1. Lilljebjorn H, Fioretos T. New oncogenic subtypes in pediatric B-cell precursor acute lymphoblastic leukemia. Blood. 2017;130(12):1395-1401.
2. Malard F, Mohty M. Acute lymphoblastic leukaemia. Lancet. 2020;395(10230):1146-1162.
3. Gokbuget N, Boissel N, Chiaretti S, et al. Diagnosis, prognostic factors, and assessment of ALL in adults: 2024 ELN recommendations from a European expert panel. Blood. 2024;143(19):1891-1902.
4. Inaba H, Mullighan CG. Pediatric acute lymphoblastic leukemia. Haematologica. 2020;105(11):2524-2539.
5. Mertens F, Johansson B, Fioretos T, Mitelman F. The emerging complexity of gene fusions in cancer. Nat Rev Cancer. 2015;15(6):371-381.
6. Ren R. Mechanisms of BCR-ABL in the pathogenesis of chronic myelogenous leukaemia. Nat Rev Cancer. 2005;5(3):172-183.
7. Olsen SN, Godfrey L, Healy JP, et al. MLL::AF9 degradation induces rapid changes in transcriptional elongation and subsequent loss of an active chromatin landscape. Mol Cell. 2022;82(6):1140-1155.e11.
8. Guo M, Chan THM, Zhou Q, et al. Core-binding factor fusion downregulation of ADAR2 RNA editing contributes to AML leukemogenesis. Blood. 2023;141(25):3078-3090.
9. Day RB, Hickman JA, Xu Z, et al. Proteogenomic analysis reveals cytoplasmic sequestration of RUNX1 by the acute myeloid leukemia-initiating CBFB::MYH11 oncofusion protein. J Clin Invest. 2023;134(4):e176311.
10. Heikamp EB, Henrich JA, Perner F, et al. The menin-MLL1 interaction is a molecular dependency in NUP98-rearranged AML. Blood. 2022;139(6):894-906.
11. Lilljebjorn H, Henningsson R, Hyrenius-Wittsten A, et al. Identification of ETV6-RUNX1-like and DUX4-rearranged subtypes in paediatric B-cell precursor acute lymphoblastic leukaemia. Nat Commun. 2016;7:11790.
12. Mullighan CG, Collins-Underwood JR, Phillips LA, et al. Rearrangement of CRLF2 in B-progenitor- and Down syndrome-associated acute lymphoblastic leukemia. Nat Genet. 2009;41(11):1243-1246.
13. Liu J, Tokheim C, Lee JD, et al. Genetic fusions favor tumorigenesis through degron loss in oncogenes. Nat Commun. 2021;12(1):6704.
14. Stransky N, Cerami E, Schalm S, Kim JL, Lengauer C. The landscape of kinase fusions in cancer. Nat Commun. 2014;5:4846.
15. Fu Y, Dominissini D, Rechavi G, He C. Gene expression regulation mediated through reversible m(6)A RNA methylation. Nat Rev Genet. 2014;15(5):293-306.
16. Wang T, Kong S, Tao M, Ju S. The potential role of RNA N6-methyladenosine in Cancer progression. Mol Cancer. 2020;19(1):88.
17. Wang Y, Wang Y, Patel H, et al. Epigenetic modification of m(6)A regulator proteins in cancer. Mol Cancer. 2023;22(1):102.
18. Jiang X, Liu B, Nie Z, et al. The role of m6A modification in the biological functions and diseases. Signal Transduct Target Ther. 2021;6(1):74.
19. Fang Z, Mei W, Qu C, et al. Role of m6A writers, erasers and readers in cancer. Exp Hematol Oncol. 2022;11(1):45.
20. Zaccara S, Ries RJ, Jaffrey SR. Reading, writing and erasing

mRNA methylation. Nat Rev Mol Cell Biol. 2019;20(10):608-624.
21. Fang Y, Wang M, Hu S, et al. Recurrent novel P2RY8/IGH translocations in B-lymphoblastic leukemia/lymphoma. Front Oncol. 2022;12:896858.
22. Boo SH, Kim YK. The emerging role of RNA modifications in the regulation of mRNA stability. Exp Mol Med. 2020;52(3):400-408.
23. Qin B, Yu J, Nowsheen S, Zhao F, Wang L, Lou Z. STK38 promotes ATM activation by acting as a reader of histone H4 ufmylation. Sci Adv. 2020;6(23):eaax8214.
24. Song S, Mazurek N, Liu C, et al. Galectin-3 mediates nuclear β-catenin accumulation and Wnt signaling in human colon cancer cells by regulation of glycogen synthase kinase-3β activity. Cancer Res. 2009;69(4):1343-1349.
25. Besson A, Wilson TL, Yong VW. The anchoring protein RACK1 links protein kinase Cε to integrin β chains: requirement for adhesion and motility. J Biol Chem. 2002;277(24):22073-22084.
26. Rigas AC, Ozanne DM, Neal DE, Robson CN. The scaffolding protein RACK1 interacts with androgen receptor and promotes cross-talk through a protein kinase C signaling pathway. J Biol Chem. 2003;278(46):46087-46093.
27. Neary JT, Kang Y. P2 purinergic receptors signal to glycogen synthase kinase-3β in astrocytes. J Neurosci Res. 2006;84(3):515-524.
28. Tran TM, Philipp J, Bassi JS, et al. The RNA-binding protein IGF2BP3 is critical for MLL-AF4-mediated leukemogenesis. Leukemia. 2022;36(1):68-79.
29. Palanichamy JK, Tran TM, Howard JM, et al. RNA-binding protein IGF2BP3 targeting of oncogenic transcripts promotes hematopoietic progenitor proliferation. J Clin Invest. 2016;126(4):1495-1511.
30. Yang Y, Gao J, Shi H, et al. IGF2BP3 as a prognostic biomarker and regulator of metastasis in Merkel cell carcinoma. JID Innov. 2025;5(3):100355.
31. Lagadinou ED, Sach A, Callahan K, et al. BCL-2 inhibition targets oxidative phosphorylation and selectively eradicates quiescent human leukemia stem cells. Cell Stem Cell. 2013;12(3):329-341.
32. Chan SM, Thomas D, Corces-Zimmerman MR, et al. Isocitrate dehydrogenase 1 and 2 mutations induce BCL-2 dependence in acute myeloid leukemia. Nat Med. 2015;21(2):178-184.
33. Pollyea DA, Stevens BM, Jones CL, et al. Venetoclax with azacitidine disrupts energy metabolism and targets leukemia stem cells in patients with acute myeloid leukemia. Nat Med. 2018;24(12):1859-1866.
34. Stevens BM, Jones CL, Pollyea DA, et al. Fatty acid metabolism underlies venetoclax resistance in acute myeloid leukemia stem cells. Nat Cancer. 2020;1(12):1176-1187.
35. He PC, Wei J, Dou X, et al. Exon architecture controls mRNA m(6)A suppression and gene expression. Science. 2023;379(6633):677-682.
36. Hu X, Wang Q, Tang M, et al. TumorFusions: an integrative resource for cancer-associated transcript fusions. Nucleic Acids Res. 2018;46(D1):D1144-D1149.
37. Du W, Xia Z, Luo Z, et al. A novel gene fusion RUNX1/ZNF423 promotes leukemic relapse of NUP98-rearranged AML. Leukemia. 2023;37(11):2286-2291.
38. Zhang J, McCastlain K, Yoshihara H, et al. Deregulation of DUX4 and ERG in acute lymphoblastic leukemia. Nat Genet. 2016;48(12):1481-1489.
39. Li JF, Dai YT, Lilljebjorn H, et al. Transcriptional landscape of B cell precursor acute lymphoblastic leukemia based on an international study of 1,223 cases. Proc Natl Acad Sci U S A. 2018;115(50):E11711-E11720.
40. Martin AP, Aushev VN, Zalcman G, Camonis JH. The STK38-XPO1 axis, a new actor in physiology and cancer. Cell Mol Life Sci. 2021;78(5):1943-1955.
41. Han L, Dong L, Leung K, et al. METTL16 drives leukemogenesis and leukemia stem cell self-renewal by reprogramming BCAA metabolism. Cell Stem Cell. 2023;30(1):52-68.e13.
42. Li Z, Weng H, Su R, et al. FTO plays an oncogenic role in acute myeloid leukemia as a N(6)-methyladenosine RNA demethylase. Cancer Cell. 2017;31(1):127-141.
43. Huang Y, Su R, Sheng Y, et al. Small-molecule targeting of oncogenic FTO demethylase in acute myeloid leukemia. Cancer Cell. 2019;35(4):677-691.e610.
44. Wang J, Li Y, Wang P, et al. Leukemogenic chromatin alterations promote AML leukemia stem cells via a KDM4C-ALKBH5-AXL signaling axis. Cell Stem Cell. 2020;27(1):81-97.e88.
45. Shen C, Sheng Y, Zhu AC, et al. RNA demethylase ALKBH5 selectively promotes tumorigenesis and cancer stem cell self-renewal in acute myeloid leukemia. Cell Stem Cell. 2020;27(1):64-80.e69.
46. Hong YG, Yang Z, Chen Y, et al. The RNA m6A reader YTHDF1 is required for acute myeloid leukemia progression. Cancer Res. 2023;83(6):845-860.
47. Sheng Y, Wei J, Yu F, et al. A critical role of nuclear m6A reader YTHDC1 in leukemogenesis by regulating MCM complex-mediated DNA replication. Blood. 2021;138(26):2838-2852.
48. Weng H, Huang F, Yu Z, et al. The m(6)A reader IGF2BP2 regulates glutamine metabolism and represents a therapeutic target in acute myeloid leukemia. Cancer Cell. 2022;40(12):1566-1582.e1510.
49. Zhang N, Shen Y, Li H, et al. The m6A reader IGF2BP3 promotes acute myeloid leukemia progression by enhancing RCC2 stability. Exp Mol Med. 2022;54(2):194-205.
50. Shu C, Gu M-H, Zeng C, et al. Small-molecule exhibits anti-tumor activity by targeting the RNA m6A reader IGF2BP3 in ovarian cancer. Am J Cancer Res. 2023;13(10):4888.